Nanoscale Horizons

ROYAL SOCIETY OF CHEMISTRY

COMMUNICATION

View Article Online
View Journal | View Issue

Cite this: *Nanoscale Horiz.*, 2024, 9, 1766

Received 31st March 2024,
Accepted 23rd July 2024

DOI: 10.1039/d4nh00137k

rsc.li/nanoscale-horizons

Freestanding monolayer CrOCl through chemical exfoliation†

Graciela Villalpando,[a] Jiaze Xie,[a] Nitish Mathur,[a] Guangming Cheng,[a] Nan Yao[b] and Leslie M. Schoop *[a]

Magnetic two-dimensional (2D) materials are a unique class of quantum materials that can exhibit interesting magnetic phenomena, such as layer-dependent magnetism. The most significant barrier to 2D magnet discovery and study lies in our ability to exfoliate materials down to the monolayer limit. Therefore designing exfoliation methods that produce clean, monolayer sheets is crucial for the growth of 2D material research. In this work, we develop a facile chemical exfoliation method using lithium naphthalenide for obtaining 2D nanosheets of magnetic van der Waals material CrOCl. Using our optimized method, we obtain freestanding monolayers of CrOCl, with the thinnest measured height to date. We also provide magnetic characterization of bulk, intercalated intermediate, and nanosheet pellet CrOCl, showing that exfoliated nanosheets of CrOCl exhibit magnetic order. The results of this study highlight the tunability of the chemical exfoliation method, along with providing a simple method for obtaining 2D CrOCl.

New concepts

Magnetic two-dimensional (2D) materials are a relatively new and integral class of quantum materials that are highly sought after for both research and real-life application purposes. Despite the significance, the current library of existing air-stable magnetic monolayers is extremely limited. CrOCl, an antiferromagnet rich in magnetic features, is one of many magnetic materials yet to be exfoliated to produce freestanding monolayers. Chemical exfoliation, a top-down solution based method, has not only shown promise in producing freestanding monolayers, but has produced air-stable monolayers of magnetic materials in previous studies. In this work we provide a facile chemical exfoliation method using lithium naphthalene to produce freestanding air-stable monolayers of CrOCl for the first time. Our results provide infrastructure for future studies on monolayer CrOCl. We also provide the thinnest atomic force microscopy measurements of monolayer CrOCl obtained thus far and show how the chemically exfoliated sheets can be cleaned. We hope that this work highlights the adaptability of chemical exfoliation for difficult materials, and bolsters research into chemical exfoliation as a tool to expand the number of existing magnetic monolayers.

1 Introduction

Two-dimensional (2D) magnets are an integral component in the advancement of spintronics and nano-technology.[1,2] First discovered in 2017 with monolayer CrI_3, magnetic 2D materials demonstrated the ability to tune the magnetism of a material through layer number.[3,4] Having the advantages of being atomically thin and magnetic tunability has established 2D magnets as highly versatile, both as stackable building blocks for devices and simple models for studying exotic magnetic properties.[5–7] Consequentially, 2D magnets are a valuable resource for both applications and fundamental study. The utility of 2D magnets has greatly catalyzed the field of low-dimensional materials; however, obtaining free-standing monolayers of many magnetic materials of interest has proven difficult. While traditional mechanical exfoliation methods, such as the Scotch tape method, are generally the first choice for obtaining 2D materials, it is confined to materials with only very weak interlayer interactions, and often does not result in free-standing monolayers.[8] Therefore, developing alternative methods to obtain clean, air stable 2D magnets is necessary for the advancement of 2D material production and application.

Recently, chemical exfoliation, an alternative to mechanical exfoliation, has been proved a useful method for obtaining 2D or even 1D (one-dimensional) materials where traditional mechanical methods fail.[5,9–11] Similar to Scotch tape exfoliation, chemical exfoliation is a top-down method typically used for layered bulk materials. One of the common chemical exfoliation approaches takes advantage of redox chemistry to intercalate (or deintercalate) ions or molecules between the layers of the materials of interest, weakening the interlayer

[a] *Department of Chemistry, Princeton University, Princeton, NJ 08544, USA. E-mail: lschoop@princeton.edu*
[b] *Princeton Materials Institute, Princeton, NJ 08544, USA*

† Electronic supplementary information (ESI) available. See DOI: https://doi.org/10.1039/d4nh00137k

interactions.[5,12,13] Thereafter, shear forces such as shaking and/or sonication are applied to delaminate the layers, creating a 2D nanosheet suspension. The merit of this method lies in the tunability of each step, allowing for exfoliation of more complicated materials. For example, the choice of intercalent and the involved chemistry for insertion between the layers of the host material has been shown to have an immense affect on the success of the exfoliation.[14,15] It is highly dependent on the reduction potential of the intercalent compared to the host material.[15,16] Other factors, such as the solvents used for shaking, timing, and sonication parameters have been shown to impact the quality of exfoliation as well.[10,14,17,18]

Transition metal oxychlorides (TMOCl) are van der Waals layered compounds in the space group *Pmmn*. This family has proven valuable as cathode materials for batteries, in addition to exhibiting interesting electronic and magnetic properties such as magnetic anisotropy and Mott insulator behaviour.[19–21] Unlike other van der Waals materials, the conventional mechanical methods are not efficient for the exfoliation of TMOCl compounds to the monolayer limit. Recently, by using wet chemical treatments, our lab has reported the successful isolation of monolayers or nanosheets of FeOCl and VOCl, which retained their magnetic order.[10,22] The methodology developed from the previous work should be also suitable for other members of TMOCl family, allowing us to continues the exploration of more interesting low-dimensional magnetism.

CrOCl has captured interest in the 2D materials community due to the complex magnetic features of the bulk phase. This compound is an insulating antiferromagnet with in-plane anisotropy and highly complex magnetic interactions. Previous studies have shown that CrOCl has a Néel temperature of approximately 13.6 K associated with a monoclinic distortion to $P2_1/m$ and an additional phase transition below 30 K due to an incommensurate magnetic state, as found by magnetic, heat capacity, and neutron measurements.[23,24] Additionally, recent work using dynamic cantilever magnetometry reports a rich magnetic phase diagram of bulk CrOCl with four total magnetic phase transitions: antiferromagnetic, ferrimagnetic, incommensurate, and paramagnetic.[25] The intriguing magnetism found in the bulk has cultivated significant interest in using monolayer CrOCl for strain tuned and spintronic devices.[26,27] Furthermore, theoretical predictions on the magnetic character of monolayer CrOCl are ambiguous, having been calculated to be both ferromagnetic and antiferromagnetic in separate studies, making experimental studies on monolayer CrOCl valuable for refining theoretical studies as well.[28,29] In literature, although this compound has been exfoliated mechanically down to the monolayer limit and monolayer edges have been obtained, freestanding monolayers of CrOCl have yet to be obtained.[30] The lack of studies on freestanding monolayers makes it difficult to corroborate the ferromagnetic theoretical predictions.[28,31] Taken all together, an alternative exfoliation method is necessary for decent studies of interesting 2D magnets.

While in previous studies, monolayers of other members of the TMOCl family are successfully obtained by treating with *n*-butyllithium,[10,22] a common reducing agent, we found that *n*-butyllithium was not reducing enough to be effective for CrOCl. This is most likely due to the stable oxidation state of Cr^{3+} (low Cr^{3+}/Cr^{2+} redox potential). Thus, we shift our attention to lithium naphthalenide, one of the most reducing organic agents, as a lithiation reagent, as shown in Fig. 1. In fact, alkali naphthalenide compounds are widely used in organometallic chemistry, and have historically been tested for solid-state intercalation chemistry.[32,33] Additionally, previous studies by Zheng *et al.* have had success in chemically exfoliating MoS_2 down to the monolayer level using alkali naphthalenides as an intercalant. Compared to *n*-butyllithium, naphthalenide salts are not only stronger reductants but also provide reversible redox reactions, namely leading to innocent and soluble naphthalene as final products. Despite these advantages, the use of lithium naphthalenide in a chemical exfoliation based synthesis of 2D transition metal oxychlorides has not been reported to our knowledge. In this study, by using lithium naphthalenide-based intercalation, followed by shaking and sonication, we successfully obtained freestanding CrOCl

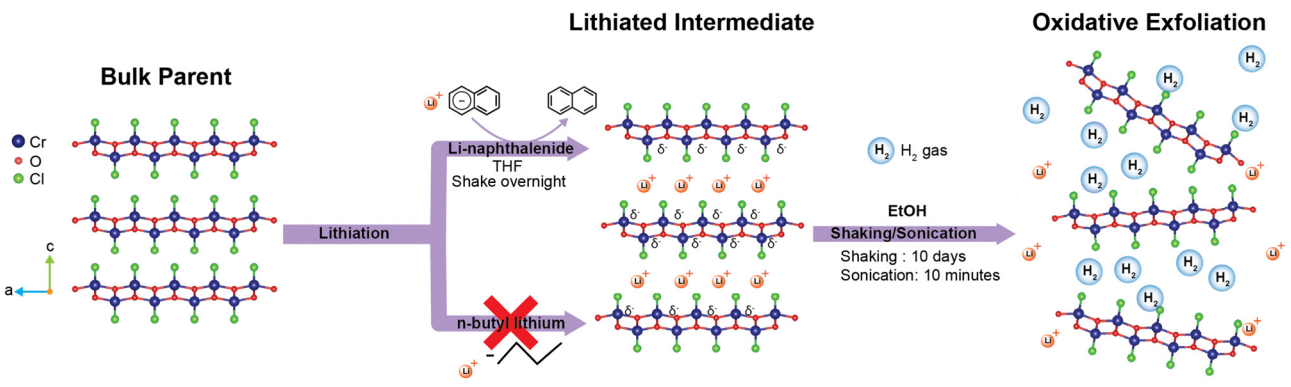

Fig. 1 General scheme for the exfoliation of CrOCl. Bulk CrOCl is first treated with a lithium naphthalenide solution, intercalating lithium within the layers. Treating CrOCl with *n*-butyl lithium does not result in a successful intercalation. The resulting intermediate from the lithium naphthalenide solution is then shaken in ethanol, oxidizing the lithiated product, removing the intercalated lithium, and producing hydrogen bubbles. Sonication of the resulting product delaminates the CrOCl, producing a 2D nanosheet suspension.

monolayers. Furthermore, we establish a simple route to cleaning chemically exfoliated nanosheets, addressing the issue of chemical exfoliation producing "dirty"surfaces.[5] The resulting product contains monolayers with a height of 0.75 nm after cleaning, which are the thinnest sheets of CrOCl reported to date and the only freestanding monolayers to our knowledge. In addition, some magnetic characterizations are carried out for both fresh-made bulk materials and restacked nanosheet pellets.

2 Results and discussion

2.1 Bulk characterization

Parent crystals of CrOCl were grown as described in the "Methods" section below. Crystals appear shiny black and are air stable. CrOCl parent crystals were intercalated with lithium using lithium naphthalenide in a modified version from Zheng *et al.*[14] Specifically, we do not need to pre-expand the layers using hydrazine as described in Zheng *et al.* CrOCl is combined with a 0.1 M lithium naphthalenide solution and shaken for 24 hours under argon. The solid is then removed, rinsed with additional THF, and then dried under argon. Further description can be found in the "Methods" section. We note that we attempted both sodium naphthalenide and lithium naphthalenide, and although both appeared to be intercalated successfully, only samples using lithium naphthalenide as the reductant were able to be exfoliated under the conditions demonstrated here. Successfully lithiated CrOCl crystals appear matte black, and violently react with EtOH forming hydrogen bubbles.

The crystallinity of both the parent and the lithiated intermediate were assessed with powder X-ray diffraction (PXRD) as shown in Fig. 2. The parent pattern shows pure, crystalline CrOCl. The lithiated intermediates PXRD pattern indicates successful intercalation of lithium. The large peaks at low angles and the smaller peak at 4.43° (labeled with purple asterisks in Fig. 2) represent the expansion of the interlayer distance attributed to intercalation of both lithium and solvated lithium.[34] The larger peak labeled with a purple asterisk at approximately 2.23° represents an increase of the interlayer gallery distance from approximately 0.78 nm in the parent to 1.12 nm, which is consistent with other Li-THF intercalated materials.[35] The reflection located at 4.43° is possibly a disparity in solvent intercalation in the interlayer spacing throughout the crystal, and more closely resembles the intercalation of a non-solvated lithium ion based on the much smaller increase of interlayer distance (interlayer distance equal to 0.92 nm). However, the main peaks at 11.8° and 21.24° are still retained. Additional reflections (labeled with green triangles in Fig. 2) are consistently in the lithiated batches, however cannot be easily explained based on the quality of the data. The drastic shifting of the (001) peak and peak broadening are characteristic of successful intercalation of lithium. This is further supported by inductively coupled plasma optical emission measurements (ICP-OES) (Table S1 in the ESI†), indicating approximately a 1 : 1 molar ratio of chromium to lithium in the lithiated intermediate.

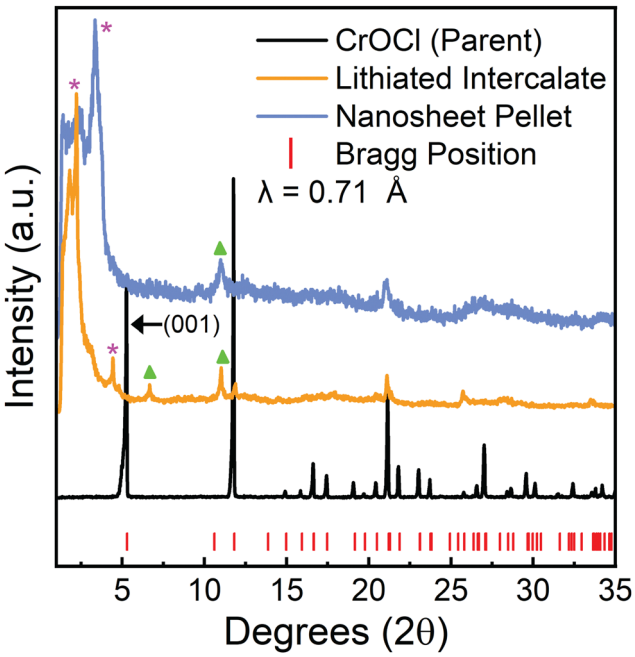

Fig. 2 Powder X-ray diffraction patterns of the parent CrOCl (black), lithiated intermediate (orange), and nanosheet (NS) pellet (blue) with the Bragg positions (red) taken from ICSD collection code 4086 for comparison. The stacking peak in the parent compound, labeled (001), is indicated with an arrow. Peaks labeled with a purple asterisk represent the interlayer stacking peaks shifted from the original (001) peak found in the parent. Peaks labeled with a green triangle indicate additional reflections not found in the parent compound.

2.2 Nanosheet characterization

Nanosheets of CrOCl were synthesized by exfoliating the lithiated intermediate by shaking the lithiated intermediate in EtOH for ten days followed by 10 minutes of sonication, as described in the "Methods" section. Nanosheets, nanosheet suspensions, and nanosheet pellets appear to be air stable. Sheets in suspension contain a slight negative charge of approximately −17.63 mV, as measured by ζ potential.

Nanosheet pellets were obtained from nanosheet suspensions as described in the "Methods" section below. The large low-angle peak (labeled with a purple asterisk, Fig. 2) is slightly shifted towards higher angles compared to that of the lithiated intermediate, indicating a decrease in interlayer stacking distance. This peak also contains the Warren-type tailing towards higher angles often seen in turbostratically restacked nanosheets.[36] However, a large background still exists at all angles below this peak. This is common for restacked nanosheets and stems from the large spacing between the randomly restacked nanosheets.[34] Additionally, a peak not found in the parent (labeled with a green triangle, Fig. 2) is retained from the lithiated intermediate along with a peak at approximately 21.24° that matches both the intermediate and parent compound. However, the quality of the PXRD from the nanosheet

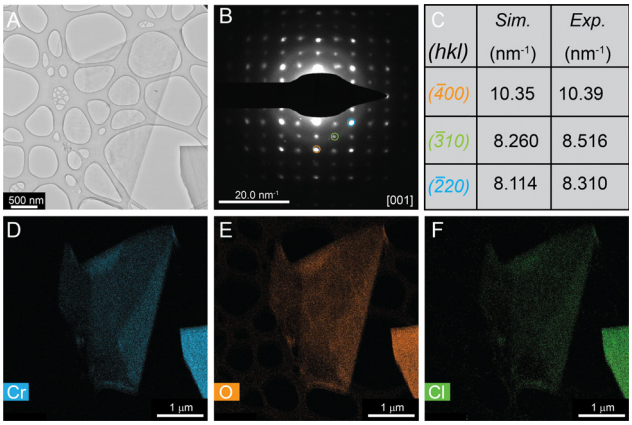

Fig. 3 (A) Transmission electron microscopy image of CrOCl nanosheets, with corresponding (B) diffraction pattern, (C) measured reciprocal length from (B) and simulated reciprocal length of selected points, and (D)–(F) energy dispersive X-ray spectroscopy maps of a nanosheet showing (D) Cr, (E) O, and (F) Cl. These were the only elements detected other than the the carbon and copper stemming from the TEM grid.

pellet prevents accurate structural analysis. Further structural information of the nanosheets can be found in the diffraction obtained from transmission electron microscopy (TEM) (Fig. 3 and Fig. S1 and S2, ESI†) and the high resolution scanning transmission electron microscopy (HRSTEM) (Fig. S3, ESI†).

TEM of these chemically exfoliated CrOCl nanosheets reveals large amounts of clean and thin sheets (Fig. 3, Fig. S1 and S2, ESI†). Energy-dispersive X-ray spectroscopy (EDX) demonstrates that these sheets contain chromium, oxygen, and chlorine as indicated by Fig. 3D–F below. Selected area electron diffraction (SAED) reveals that these nanosheets are also highly crystalline (Fig. 3B). Compared to that of the simulated bulk CrOCl pattern, the CrOCl nanosheets contain similar *d*-spacing distances (Fig. 3C). However, CrOCl nanosheet diffraction patterns also contain additional peaks that are forbidden for the parent space group (*Pmmn*) (as shown in Fig. S2, ESI†). This is very similar to our previous study on the nanosheets of chemically exfoliated VOCl, which showed the same diffraction pattern when exfoliated down to lower dimensions.[10] These additional spots could mark a shift from orthorhombic to monoclinic, a requirement for in-plane antiferromagnetic ordering seen at lower temperatures in this compound.[23,37] Alternatively, this could be a consequence of the low dimensionality of the sheets, a phenomenon that has been observed in multiple low-dimensional systems.[38,39] Diffraction patterns were also obtained with increasing temperature from 25 °C to 500 °C (Fig. S3, ESI†), but no changes in the pattern were observed. This implies that the structure of these sheets is extremely robust. Additional TEM and diffraction of CrOCl nanosheets can be found in Fig. S1–S4 (ESI†).

Thickness of nanosheets obtained from the chemically exfoliated CrOCl were measured using atomic force microscopy. Atomic force microscopy measurements of a CrOCl monolayer can be found in Fig. 4 showing that a layer of CrOCl is approximately 1.15 nm per layer, which is further corroborated by the folded portion showing a step of approximately 1.16 nm and a roughness of 154.4 pm. The height from substrate to sheet of the monolayer, not being the expected height of a single layer CrOCl, is due to solvent and water absorption on the surfaces of both the sheet and substrate.[36] Our sheet is thinner than previous studies of mechanically exfoliated monolayer CrOCl edges on SiO_2 substrates (1.40 nm), further supporting evidence that we achieved the monolayer limit.[30] A additional height measurement of a bilayer (Fig. S5, ESI†) is measured to be 1.80 nm, agreeing with previous studies of the CrOCl layer to layer distance being approximately 0.80 nm.[30] The optical microscope images of these nanosheets along with additional sheets can be found in Fig. S6 (ESI†). A histogram showing the typical lateral size distribution of nanosheets made with this method are also included in Fig. S7 (ESI†).

In order to show the stability of the chemically exfoliated CrOCl sheets, another height measurement was conducted on the same monolayer left in ambient conditions nineteen days later. The height of this monolayer was measured to be 1.68 nm (Fig. 5) with a roughness of 107.4 pm. The increase in height

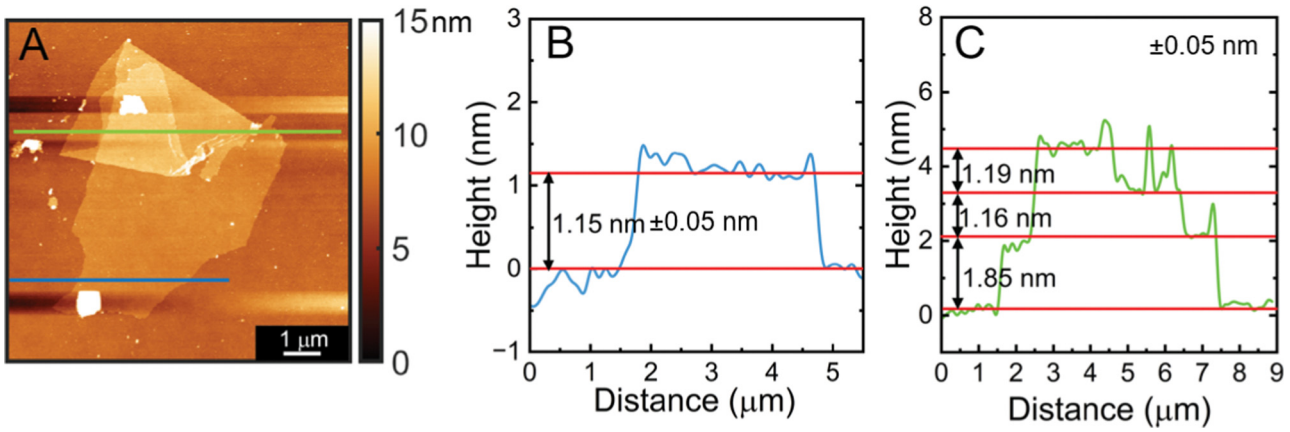

Fig. 4 Atomic force microscopy measurement of the monolayer CrOCl shown in (A). Panel (B) and (C) show the height of a monolayer to be approximately 1.15 nm.

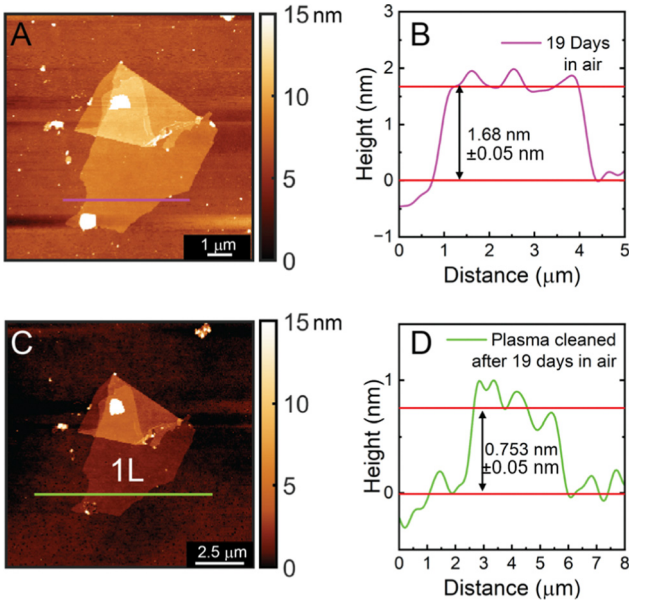

Fig. 5 Height measurements for the same monolayer shown in Fig. 4 after 19 days in air (A) and (B) and after 19 days in air with 1 minute of plasma cleaning with O_2 (C) and (D).

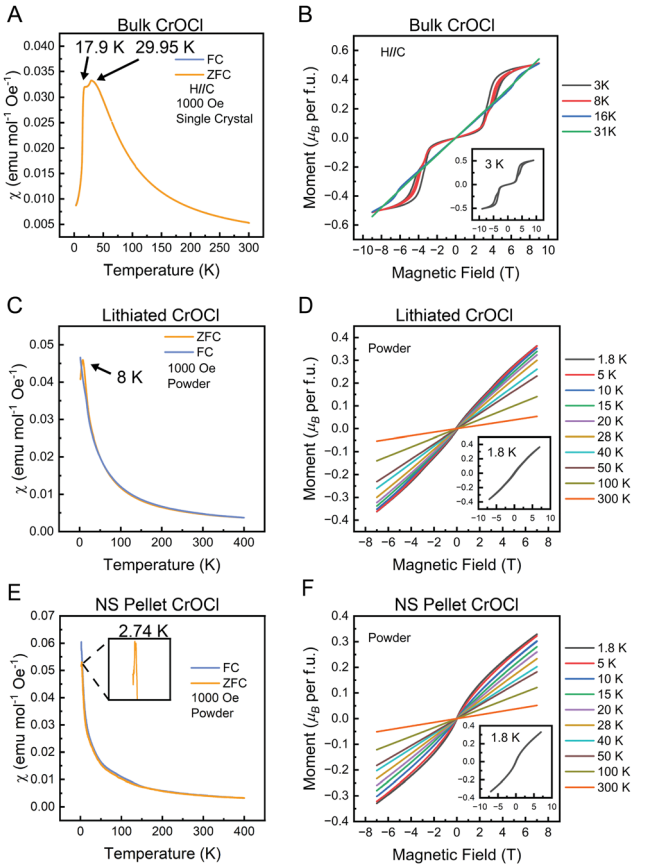

Fig. 6 Magnetic characterization of (A) and (B) bulk CrOCl, (C) and (D) lithiated CrOCl intermediate, and (E) and (F) nanosheet (NS) pellet of CrOCl. The transition temperature for NS pellet CrOCl (E) is shown in the zoomed in inset showing the transition temperature to be 2.74 K. Insets in (B), (D), and (F) depict the moment *versus* field measured at the lowest temperature for each step.

and decrease in roughness is due to additional absorption of water and hydrocarbons on the surface of the sheet over time. To support this, an additional measurement was taken after plasma cleaning the same monolayer for one minute. The plasma-cleaned monolayer has a height of 0.75 nm and a roughness of 146.3 pm, the thinnest monolayer measurement of CrOCl obtained thus far and close to the approximated layer to layer distance of 0.80 nm. This is also significantly closer to the measured monolayer distance obtained from the crystal model of CrOCl (0.64 nm). HRSTEM images of pre-plasma cleaned sheets also show an amorphous layer on the surface of the sheets (Fig. S3B, ESI†). Overall, these measurements conclude that the chemically exfoliated CrOCl sheets are not air sensitive, and plasma cleaning can be a valuable tool in obtaining clean sheet surfaces and accurate atomic force microscopy height measurements without hydrocarbon or water contribution.

2.3 Magnetic characterization

The magnetic properties of the bulk parent, lithiated intermediate, and nanosheet (NS) pellet were measured, as presented in Fig. 6. Stacked bulk CrOCl crystals were used for measurements with the field applied along the stacking axis, which shows two transitions at approximately 17.90 K and 29.95 K, similar to the results in previous reports.[24] The field *versus* moment plots (Fig. 6B) show the characteristic metamagnetic steps with hysteresis at low temperatures.

The lithiated intermediate shows a drastic change in the magnetic character compared to the bulk parent. The susceptibility measurement shows a single transition at 8 K, indicating the loss of the higher-temperature transition associated with the structural change. The field *versus* moment plots only show a soft "S-shape" at low temperatures (Fig. 6D inset), in addition to the loss of the metamagnetic steps found in the bulk.

The restacked NS pellet magnetic data is complementary to the lithiated intermediate, with a single magnetic transition and only a soft "S-shape" at low temperatures for the field *versus* moment data. However, the magnetic transition is further decreased to 2.74 K (Fig. 6E inset). The Curie–Weiss fit (Fig. S8, ESI†) indicates a Curie–Weiss temperature of −42.26 K, implying antiferromagnetic interactions and a calculated μ_{eff} of $3.35\mu_B$. The latter value is close to the expected value of $3.87\mu_B$ for spin-only Cr^{3+}.

The absence of the second, higher transition temperature in both the lithiated intermediate and restacked NS pellet most likely stems from the lack of a structural transition. Based on the similar XRD patterns for both the lithiated intermediate and restacked nanosheet pellet (Fig. 2), and the SAED for the nanosheets (Fig. 3B and C), we can infer that the intermediate and nanosheets have monoclinic symmetry, thereby eliminating the structural transition usually seen in bulk CrOCl, thus destroying the higher temperature magnetic transition. The lack of hysteresis and metamagnetic steps in both the lithiated intermediate and the restacked NS pellet could be a

consequence of these measurements being performed with no field orientation. The magnetic properties of bulk CrOCl are highly anisotropic, therefore the lack of field orientation could suppress hysteresis in the lithiated and restacked NS pellet measurements. Another possibility is the decrease in interlayer interactions in the lithiated intermediate and the restacked NS pellet could have broken the magnetic ordering that leads to these features in the bulk. Since the bulk only shows these metamagnetic features with the field aligned along the stacking axis, either of these arguments could contribute to the loss of the characteristic metamagnetic steps and hysteresis loops. Although our measurements were not performed on CrOCl monolayers, the magnetic characterization of the restacked NS pellet still shows a magnetic moment high enough to imply that the whole sample is contributing to the magnetism. Additionally, the magnetic transition obtained appears to be highly air stable, even after measuring another restacked nanosheet pellet exposed to air and bromine for over 24 hours (Fig. S9, ESI†). The results support that the exfoliated sheets are still magnetic. Certainly, in order to obtain a more comprehensive characterization of the magnetic nature of 2D/monolayer CrOCl, careful measurements on a single monolayer of CrOCl will be required, such as magneto optical Kerr effect (MOKE) measurements.

3 Conclusions

In this work, the magnetic van der Waals compound CrOCl was exfoliated using an optimized chemical exfoliation method. This method uses lithium naphthalenide, a reducing agent, to insert lithium in between the layer of the bulk material. This not only leads to an expansion of the interlayer distance, but allows the ethanol shaking solution to re-oxidize the bulk material, removing the lithium from in between the layers and producing hydrogen bubbles, further weakening the interlayer forces. Shaking/sonication of the resulting suspension easily exfoliates the layers into a 2D nanosheet suspension. The resulting free-standing CrOCl monolayers are confirmed by atomic force microscopy, which have not been previously obtained. Furthermore, comprehensive characterization of TEM, HRSTEM, EDX, and SAED suggests that chemically delaminated CrOCl nanosheets are highly crystalline. Additionally, magnetic characterization was performed on all three-stages of materials (bulk, lithiated intermediate, and restacked NS pellet), showing that the restacked nanosheet pellet remains magnetic. The obtained free-standing monolayers of CrOCl could be used for more in-depth magnetic study at atomic level. These promising results demonstrate the universality of wet-chemical methodology and its potential for wide-range layered materials. The interdisciplinary lessons underpins the more versatile chemical based exfoliation, paving the way to the development of 2D quantum materials.

4 Methods

4.1 Bulk synthesis

CrOCl crystals were grown using a modified chemical vapor transport (CVT) method taken from Zhang *et al.*[24] $CrCl_3$ (Sigma Aldrich, 99%) and Cr_2O_3 (Sigma Aldrich, 98%) were ground together and pressed into a pellet in a 1 : 1 molar ratio. The pellet was vacuum-sealed in a quartz ampoule and placed in a tube furnace. The furnace was heated to 940 °C over 16 hours, held at this temperature for 170 hours, and then cooled to room temperature over 16 hours. The bulk CrOCl crystals are typically 1–3 mm long.

4.2 Lithium intercalation

Lithiation using lithium naphthalenide was conducted using a modified version of the method used in Zheng *et al.*[14] The lithium naphthalenide solution was made in an inert environment under argon at room temperature. All glassware was dried before use. Excess elemental lithium (Sigma Aldrich, 99%) and naphthalene (Sigma Aldrich, 99%) were combined in a 2.05 : 1 molar ratio in THF (Sigma Aldrich, anhydrous, inhibitor free, ≥99.99%) to make a 0.1 M lithium naphthalenide solution followed by shaking overnight. Intercalation was achieved by adding CrOCl crystals in a 1 : 2 molar ratio of CrOCl : Li-naphthalenide to the Li-naphthalenide solution. The suspension containing CrOCl was shaken for 24 hours, resulting in dark black crystals. The crystals were rinsed with additional THF and vacuum dried. Lithiated crystals were stored in the glovebox.

4.3 Chemical exfoliation

Lithiated CrOCl crystals were removed from the glovebox and quickly added to a centrifuge tube with EtOH which results in rapid bubbling. This CrOCl containing suspension was then shaken for 10 days at 300 revolutions per minute (rpm) under ambient conditions. It should be noted that although 10 days of shaking was found to produce 2D sheets, it could be possible that a shorter amount of shaking time will produce similar results. The suspension was then centrifuged at 10 000 for 10 minutes, supernatent removed, and fresh EtOH added to the tube. The suspension was then sonicated for 10 minutes, leading to a nanosheet suspension. This suspension was centrifuged at 1000 rpm for 10 minutes, followed by centrifuging the supernatent for an additional 10 minutes at 2000 rpm. The supernatent resulting from the previously mentioned centrifuging step was used to measure the ζ potential of the nanosheets. This supernatent was also centrifuged at 10 000 rpm for 10 minutes to create the nanosheet pellets used for PXRD and MPMS measurements. Sheets on wafers used for cleaned atomic force microscopy measurements were plasma cleaned with O_2 for one minute.

4.4 Instrumentation and characterization

PXRD patterns were obtained from a STOE STADI P powder diffractometer with Mo-Kα_1 radiation and a Dectris Mythen 2R 1K detector, in the 2θ range from 1 to 45 degrees. The PXRD pattern used for comparison was taken from the ICSD collection code: 4086. Lithium content was measured using an Agilent 5800 ICP-OES. A Scilogex SK-0330-Pro set to 300 rpm was used to shake lithium naphthalenide and all samples. Sonication was done in a Bransonic® Ultrasonic Baths, CPX

Series, model 1800, 120 V, bath sonicator on low power (49 W) optical images of nanosheets were taken on a Leica DM2700 M optical microscope. The Talos F200X scanning/transmission electron microscope (S/TEM) with SuperX EDX (energy dispersive X-ray) detector was used obtain images of nanosheets along with EDX and selected area diffraction patterns (SAED). HRSTEM images were taken on the Titan Cubed Themis 300 double Cs-corrected scanning/transmission electron microscope (S/TEM). Diffraction patterns taken on the HRSTEM were heated from 25° to 500° on a Gatan double tilt heating holder, model 652. Before taking images the temperature was allowed to stabilize for 10 minutes. Sheet thickness was measured with the Bruker dimension edge with scan asyst atomic force microscope in tapping mode. Model monolayer thickness was measured by exporting the ionic crystal model of CrOCl from VESTA (collection code: 4086) into ImageJ, and measuring a monolayer. The plasma cleaner used to clean nanosheets was the PE-50 from PLASMA ETCH INC. Height plots were smoothed with fast Fourier transform (FFT) using 5 points. CrystalMaker software SingleCrystal was used to simulate diffraction patterns of CrOCl. Magnetic measurements of the bulk parent were taken on a quantum design DynaCool PPMS using the VSM option using the quartz holder. Magnetic measurements were performed on both the lithiated intermediated and the restacked nanosheet pellet in a SQUID-VSM magnetic property measurement system 3 (quantum design) using quartz holders with powder capsules attached using GE Varnish. The ζ potential was measured using a Mobius (Wyatt technology) ζ potential detector. CrOCl nanosheets suspended in EtOH were measured at room temperature with a voltage amplitude of 3 V and a field frequency of 10 Hz. A Huckel approximation was used for calculating the ζ potential measurements. Five measurements were taken and averaged to approximately −17.63 mV.

Data availability

Raw data is available from the corresponding author on reasonable request.

Conflicts of interest

There are no conflicts to declare.

Acknowledgements

This study was primarily supported by the DOD's office of naval research (ONR) (award number N00014-21-1-2733), the Princeton Center for Complex Materials, a National Science Foundation (NSF)-MRSEC program (DMR-2011750) and the Gordon and Betty Moore Foundation'S EPIQS initiative (grant number GBMF9064). Additional support was provided by the Princeton Catalysis Initiative (PCI) and the Packard foundation, which funded equipment purchases. The authors acknowledge the use of Princeton's Imaging and Analysis Center, which is partially supported by the Princeton Center for Complex Materials, a National Science Foundation (NSF)-MRSEC program (DMR-2011750). We would also like to acknowledge the assistance of Sanfeng Wu for allowing us to use his atomic force microscope for this work.

References

1 M. Mi, H. Xiao, L. Yu, Y. Zhang, Y. Wang, Q. Cao and Y. Wang, *Mater. Today Nano*, 2023, 100408.
2 W. Li, W. Zhu, G. Zhang, H. Wu, S. Zhu, R. Li, E. Zhang, X. Zhang, Y. Deng and J. Zhang, *et al.*, *Adv. Mater.*, 2023, **35**, 2303688.
3 B. Huang, G. Clark, E. Navarro-Moratalla, D. R. Klein, R. Cheng, K. L. Seyler, D. Zhong, E. Schmidgall, M. A. McGuire and D. H. Cobden, *et al.*, *Nature*, 2017, **546**, 270–273.
4 C. Gong, L. Li, Z. Li, H. Ji, A. Stern, Y. Xia, T. Cao, W. Bao, C. Wang and Y. Wang, *et al.*, *Nature*, 2017, **546**, 265–269.
5 X. Song, F. Yuan and L. M. Schoop, *Appl. Phys. Rev.*, 2021, **8**, 011312.
6 A. Gupta, T. Sakthivel and S. Seal, *Prog. Mater. Sci.*, 2015, **73**, 44–126.
7 K. S. Burch, D. Mandrus and J.-G. Park, *Nature*, 2018, **563**, 47–52.
8 N. Mounet, M. Gibertini, P. Schwaller, D. Campi, A. Merkys, A. Marrazzo, T. Sohier, I. E. Castelli, A. Cepellotti and G. Pizzi, *et al.*, *Nat. Nanotechnol.*, 2018, **13**, 246–252.
9 T. Taniguchi, L. Nurdiwijayanto, R. Ma and T. Sasaki, *Appl. Phys. Rev.*, 2022, **9**, 021313.
10 G. Villalpando, A. M. Ferrenti, R. Singha, X. Song, G. Cheng, N. Yao and L. M. Schoop, *ACS Nano*, 2022, **16**, 13814–13820.
11 M. Yang, G. Cheng, N. Mathur, R. Singha, F. Yuan, N. Yao and L. M. Schoop, *Nanoscale Horiz.*, 2024, **9**, 479–486.
12 V. Nicolosi, M. Chhowalla, M. G. Kanatzidis, M. S. Strano and J. N. Coleman, *Science*, 2013, **340**, 1226419.
13 H. Tao, Y. Zhang, Y. Gao, Z. Sun, C. Yan and J. Texter, *Phys. Chem. Chem. Phys.*, 2017, **19**, 921–960.
14 J. Zheng, H. Zhang, S. Dong, Y. Liu, C. Tai Nai, H. Suk Shin, H. Young Jeong, B. Liu and K. Ping Loh, *Nat. Commun.*, 2014, **5**, 2995.
15 X. Zhu, Z. Su, C. Wu, H. Cong, X. Ai, H. Yang and J. Qian, *Nano Lett.*, 2022, **22**, 2956–2963.
16 D. Murphy and P. Christian, *Science*, 1979, **205**, 651–656.
17 A. Kaur and R. C. Singh, *Fullerenes, Nanotubes Carbon Nanostruct.*, 2017, **25**, 318–326.
18 A. Jawaid, D. Nepal, K. Park, M. Jespersen, A. Qualley, P. Mirau, L. F. Drummy and R. A. Vaia, *Chem. Mater.*, 2016, **28**, 337–348.
19 Y. Zeng, P. Gu, Z. Zhao, B. Zhang, Z. Lin, Y. Peng, W. Li, W. Zhao, Y. Leng and P. Tan, *et al.*, *Adv. Mater.*, 2022, **34**, 2108847.
20 M. Wu, X. Lv, J. Wang, R. Wang, X. Shi, H. Zhang, C. Jin, Y. Wei and R. Lian, *J. Mater. Chem. A*, 2021, **9**, 23169–23177.
21 S. Glawion, M. Scholz, Y.-Z. Zhang, R. Valent, T. Saha-Dasgupta, M. Klemm, J. Hemberger, S. Horn, M. Sing and R. Claessen, *Phys. Rev. B: Condens. Matter Mater. Phys.*, 2009, **80**, 155119.

22 A. M. Ferrenti, S. Klemenz, S. Lei, X. Song, P. Ganter, B. V. Lotsch and L. M. Schoop, *Inorg. Chem.*, 2019, **59**, 1176–1182.
23 P. Gu, Y. Sun, C. Wang, Y. Peng, Y. Zhu, X. Cheng, K. Yuan, C. Lyu, X. Liu and Q. Tan, *et al.*, *Nano Lett.*, 2022, **22**, 1233–1241.
24 T. Zhang, Y. Wang, H. Li, F. Zhong, J. Shi, M. Wu, Z. Sun, W. Shen, B. Wei and W. Hu, *et al.*, *ACS Nano*, 2019, **13**, 11353–11362.
25 F. Xu, H. Li, N. Wang, W. Wang, J. Xu, W. Zhu, Y. Liu, C. Zhang, Z. Qu and F. Xue, *J. Appl. Phys.*, 2023, **134**, 163904.
26 X. Qing, H. Li, C. Zhong, P. Zhou, Z. Dong and J. Liu, *Phys. Chem. Chem. Phys.*, 2020, **22**, 17255–17262.
27 C. Xu and J. Zhang, *Phys. Scr.*, 2023, **98**, 105929.
28 N. Miao, B. Xu, L. Zhu, J. Zhou and Z. Sun, *J. Am. Chem. Soc.*, 2018, **140**, 2417–2420.
29 S. W. Jang, D. H. Kiem, J. Lee, Y.-G. Kang, H. Yoon and M. J. Han, *Phys. Rev. Mater.*, 2021, **5**, 034409.
30 M. Zhang, Q. Hu, C. Hua, M. Cheng, Z. Liu, S. Song, F. Wang, P. He, G.-H. Cao, Z.-A. Xu, *et al.*, *arXiv*, 2021, preprint, arXiv:2108.02825, DOI: **10.48550/arXiv.2108.02825**.
31 Z. Guo, Y. Liu, H. Jiang, X. Zhang, L. Jin, C. Liu and G. Liu, *Mater. Today Phys.*, 2023, 101153.
32 N. G. Connelly and W. E. Geiger, *Chem. Rev.*, 1996, **96**, 877–910.
33 A. J. Jacobson and L. F. Nazar, *Encycl. Inorg. Chem.*, 2006, DOI: **10.1002/9781119951438.eibc0093**.
34 M. Acerce, D. Voiry and M. Chhowalla, *Nat. Nanotechnol.*, 2015, **10**, 313–318.
35 M. Inagaki and O. Tanaike, *Carbon*, 2001, **39**, 1083–1090.
36 D. Weber, L. M. Schoop, V. Duppel, J. M. Lippmann, J. Nuss and B. V. Lotsch, *Nano Lett.*, 2016, **16**, 3578–3584.
37 J. Angelkort, A. Wölfel, A. Schönleber, S. van Smaalen and R. K. Kremer, *Phys. Rev. B: Condens. Matter Mater. Phys.*, 2009, **80**, 144416.
38 T.-Y. Huang and C.-C. Chen, *J. Cryst. Grow.*, 2008, **310**, 853–860.
39 D. C. Bell, Y. Wu, C. J. Barrelet, S. Gradečak, J. Xiang, B. P. Timko and C. M. Lieber, *Microsc. Res. Tech.*, 2004, **64**, 373–389.